

Research Article

Volume 11 Issue 5 November 2024
DOI: 10.19080/GJPPS.2024.11.555821

Glob J Pharmaceu Sci

Copyright © All rights are reserved by Hussien M El Messiry

Essential Oil of *Foeniculum Vulgare* in Noisome Formulae Suppresses COX-II Activation in Mice Bacterial Skin Abscess Model



Hussien M. El Messiry^{1*}, Sara M. Saber², Shehab E. Talat³ and Tarek A. Ismaeel³

¹*Pharmaceutics Department, Egyptian Drug Authority (EDA formerly NODCAR) Giza, Egypt*

²*Histopathology Department, Egyptian Drug Authority (EDA formerly NODCAR) Giza, Egypt*

³*Microbiology Department, Egyptian Drug Authority (EDA formerly NODCAR) Giza, Egypt*

Submission: October 28, 2024; **Published:** November 12, 2024

***Corresponding author:** Hussien M El Messiry, Pharmaceutics Department, Egyptian Drug Authority (EDA formerly NODCAR) Giza, Egypt

Abstract

Objectives: Evaluation of niosomes formulae of *Foeniculum vulgare* oil against microbial infections caused by *E. coli* and *P. aeruginosa*.

Methods: A comparative in vivo study was done comparing the anti-inflammatory activity of *Foeniculum vulgare* oil, nisome formula, against *E. coli* and *P. aeruginosa*. This study was done in mice applying a parallel design. Mice were infected with *Pseudomonas aeruginosa* and *E. coli* bacteria. Histopathological and immunohistochemical examination, quantitative polymerase chain reaction and morphometric study were performed on mice skin after *Foeniculum vulgare* oil and noisome application.

Findings: The results indicate that nisome formula shows more efficient anti-inflammatory activity than *Foeniculum vulgare* oil.

Conclusions: Niosome formula of *Foeniculum vulgare* oil had great drug penetration and absorption besides the anti-inflammatory activity in the site of application in mice model of abscess formation was achieved by subcutaneous injection of *E. coli* and *P. aeruginosa*.

Keywords: *Foeniculum Vulgare* Oil; Noisome; COX-II; Skin Abscess Model; *Escherichia Coli*; *Pseudomonas Aeruginosa*

Abbreviations: COX: Cyclooxygenases; PG: Prostaglandin; NSAID: Nonsteroidal Anti-Inflammatory Drug; TFH: Thin-Film Hydration Method; DDW: Deionized Distilled Water; NODCAR: National Organization for Drug Control and Research; HPF: High Power Fields; PS: Particle Size; ZP: Zeta Potential; PDI: Polydispersity Index; IE: Immunoexpression; qPCR: Quantitative Polymerase Chain Reaction; SSTI: Skin and Soft Tissue Infections

Introduction

The skin is the body's largest organ, serving as a protective barrier against harmful pathogens. While this physical barrier acts as the initial line of immune defense, the skin also harbors a diverse microbial species comprised primarily of Gram-positive bacteria, such as *Corynebacteria*, *Staphylococci*, *Micrococci*, and *Propionyl* bacteria, along with the Gram-negative *Acinetobacter* [1]. These microbial species, known as commensal organisms, can live on the skin without causing harm as long as the skin remains intact. They play a protective role by competing with more harmful bacteria in various ways. Any disruption to this barrier can alter these dynamics, allowing commensal and pathogenic bacteria to infiltrate and potentially cause infections in the underlying tissues [2].

An absence is a localized accumulation of pus within body tissues, typically resulting from a bacterial infection [3]. Often, multiple bacterial types contribute to a single infection [4]. *Escherichia coli* (*E. coli*) are Gram-negative, facultative rod-shaped bacteria that normally inhabit the gastrointestinal tract. When outside their usual environment, they can lead to infections, particularly in the urinary tract, and are also linked to skin infections near the rectal area. Patients undergoing surgeries related to the gastrointestinal tract or lower spine are particularly susceptible to these infections [5,6]. *Pseudomonas aeruginosa* (*P. aeruginosa*) is a Gram-negative bacillus that can cause various opportunistic infections, especially concerning patients on ventilators, burn victims, and individuals with chronic conditions.

Skin infections associated with *P. aeruginosa* include tinea (a fungal infection), folliculitis from hot tubs or swimming pools, and sepsis from burn wounds [7]. Recent studies suggest that *P. aeruginosa*'s ability to form biofilms may contribute to chronic wounds that resist healing [8].

Cyclooxygenases (COX) are enzymes that facilitate the conversion of arachidonic acid into prostaglandin (PG), and subsequently reduce this compound to the hydroxyendoperoxide PGH2, consider a rate-limiting step in the synthesis of PG which further metabolize to numerous biologically active lipids [9]. The metabolism of arachidonic acid is crucial for human and vertebrate health, as demonstrated by the diverse applications of specific COX inhibitors. These include treatments for inflammation, allergic reactions, fever, pain, skin disorders, prevention of blood clotting, and colon cancer. A well-known nonsteroidal anti-inflammatory drug (NSAID) is acetylsalicylic acid, which inhibits COX activity, reducing the production of lipids that stimulate pain receptors, increase blood flow, and trigger inflammation [10].

There are two COX isoforms: COX-1 and COX-2. COX-1 is typically a constitutive enzyme found in various tissues, serving essential housekeeping functions, such as maintaining gastrointestinal integrity, normal kidney function, blood clotting, and wound healing. In contrast, COX-2 is an inducible enzyme whose expression increases during inflammation, seen in conditions affecting the skin, gastrointestinal tract, breast, colon, head and neck, lungs, pancreas, and under hypertonic stress [11]. *Foeniculum vulgare* has been utilized for its antifungal, antimicrobial, antioxidant, and anti-inflammatory properties [31]. A comparative *in vivo* study is done comparing the anti-inflammatory activity of *Foeniculum vulgare* oil, niosome formula, against *P. aeruginosa* and *E. coli* bacteria.

Materials and methods

Foeniculum vulgare oil (gift from Mepaco company -Egypt), span 60 and cholesterol (Sigma Aldrich- Germany), potassium dihydrogen o-phosphate and acetone (Sharlab- Spain), Nutrient agar, Eosin methylene blue agar and Cetrimide Agar (Oxoid- UK)

Preparation of Niosome Formulae

Niosomes were prepared applying Thin-Film Hydration method (TFH). Known amount of cholesterol was dissolved in acetone with stirring at 900 rpm at 40 °C using hot plate and stirrer and different amounts of span 60 dissolved in ethanol were added to cholesterol with stirring. The solution was transferred to a rotary vacuum evaporator to remove the organic solvent till a formation of a dry film on the side wall of the flask. *Foeniculum vulgare* oil (known amount dissolved in ethanol) and Phosphate buffer solution were added to the dry film at 55 °C with shaking for 24 hours. (Table 1) shows the composition of the prepared formulae.

Table 1: Prepared formulae composition.

Ingredients	F1	F2	F3
<i>Foeniculum vulgare</i> oil	25 mg	25 mg	25 mg
Cholesterol	25 mg	25 mg	25 mg
Span 60	20 mg	30 mg	40 mg
Acetone	5 mL	5 mL	5 mL
Ethanol	10 mL	10 mL	10 mL
Phosphate buffer	50 mL	50 mL	50 mL

Evaluation of the prepared formulae

The prepared formulae were evaluated for their physical appearance. The prepared niosomes were evaluated for their particle size (PI), zeta potential (ZP) and polydispersity index (PDI) as they are considered as nanoparticles.

In vivo study in mice

The best prepared niosome was chosen in order to compare its anti-inflammatory activity with *Foeniculum vulgare* oil against *Pseudomonas aeruginosa* (*P. aeruginosa*) and *Escherichia coli* (*E. coli*) bacterial infection thus improving WBCs infiltration and antibiotic activity reaching to site of infection in the further study. A parallel design was established on mice. *P. aeruginosa* and *E. coli* were isolated from food and identified by molecular technique in microbiology lab. (EDA- formally NODCAR- Giza- Egypt).

Bacterial Isolation

Preparation of *P. aeruginosa*

Ten grams of Karish cheese inoculated to 90 ml nutrient broth shake for 1 hour then take loopful into cetrizide agar then incubated at 37 °C for 24 hours for further identification.

Preparation of *E. coli*

Ten ml raw milk inoculated to 90 ml nutrient broth shake for 1 hour then take loopful into eosin methylene blue agar then incubated at 37 °C for 24 hours for further identification.

Molecular identification of *P. aeruginosa* via PCR

DNA extraction: Heat treatment was used in the DNA extraction using sterile deionized water; the bacterial cell was suspended in 100 µl sterile distilled water. The sample was immersed in a 100°C hot water bath for ten minutes. Tubes were centrifuged for 10 minutes at (13,000 rpm) 15,493×g and then supernatant fluid was removed to a sterile Eppendorf tube and freeze stored at -20°C.

Primers: *P. aeruginosa* relevant 16S r RNA primers based on Genbank database were used. Primers were Forward-(GGGGATCTTCGGACCTCA) and Reverse-(TCCTTAGAGTGCCCCACCCG).

PCR method: Conducted in a volume of 25 μ l that contained 7 μ l of deionized water, 12.5 μ l master mix, 2 μ l of each primer specific for 16SrRNA gene of *P. aeruginosa* and 2 μ l of genomic DNA from the *P. aeruginosa*, the PCR cycles were initially denatured at 95°C for 2 minutes, 25 cycles were completed, the duration of each cycle was 20 sec. at 94°C, 20 sec. at the appropriate annealing temperature (58°C) and 40 sec. at 72°C. One minute at 72°C was applied as a final extension before 30 minutes electrophoresis at 70 volt, the 1% agarose gel was stained with 2 μ l ethidium bromide and photographed under (UV) light. A 100 bp DNA ladder (MBI Ferment's USA) used as marker for the molecular weight of PCR products.

Molecular Identification of *E. coli* using PCR

DNA extraction: the same procedure of DNA extraction of *P. aeruginosa* is applied.

Primers: E coli 16Sr DNA Forward- (GGAAGAAGCTTGTCTTGTGAC) and Reverse- (AGCCCGGGGATTTCACATCTGACTTA) for 16S r DNA Primer designed based on GenBank database.

PCR method: Using Eppendorf its volume of 25 μ l containing 12.5 μ l master mix, 2 μ l of each primers specific for 16Sr DNA, 2 μ l of genomic DNA of *E. coli* isolate and 8.5 μ l of sterile deionized distilled water (DDW). The cycling conditions for amplification in a Gene Amp PCR System 9700 thermal cycler (Applied Biosystem, India) was as follows; 16Sr DNA primer initial denaturation step of 95 °C for 3 minutes followed by 30 cycles as following: (30 seconds at 95 °C for extension then 30 seconds at 55 °C for annealing, 30 seconds at 72°C for extension step) and one minute at 72°C as a final extension step. The 1% agarose gel was stained with 2 μ l ethidium bromide solution, electrophoresis at 70 volt for 30 minutes and photographed under (UV) light. The molecular weight of PCR products was determined using a 100 bp DNA ladder (MBI Ferment's USA).

Experimental Design

Thirty-five adult male albino mice weighing (30-35) grams were obtained from laboratory animal house of National Organization for Drug Control and Research (NODCAR). This was done after NODCAR Ethics Approval Committee No. 125/ 2019. Animals were kept under temperature (25±5 °C) in stainless cages. They were allowed free access to standardized diet and water and. Mice were divided into 3 groups. Group (I): 5 mice were considered as control without any treatment. Group (II): 15 mice were used and subdivided into 3 subgroups. Subgroup (II a): 5 mice were infected with *E. coli*. Subgroup (II b): 5 mice were infected with *E. coli* then treated Foeniculum vulgare oil. Subgroup (II c): 5 mice were infected with *E. coli* then treated with Foeniculum vulgare oil (Niosome form). Group (III): 15 mice were used and subdivided into 3 subgroups. Subgroup (III a): 5 mice were infected with *P. aeruginosa*. Subgroup (III b): 5 mice were infected with *P. aeruginosa* then treated with Foeniculum vulgare

oil. Subgroup (III c): 5 mice were infected with *P. aeruginosa* then treated with Foeniculum vulgare oil (Niosome form)

Histopathological examination

Skin samples were taken and fixed in 10% buffered formalin then embedded in paraffin and sectioned 5 μ m thick. Hematoxylin and eosin were used for staining these sections for the histopathological evaluation [12].

Immunohistochemical Technique

Sections of skin were deparaffinized, rehydrated in alcohol and xylene for assessment of Cyclo-oxygenase II (COX2). Antigen retrieval was done by sections incubation in citrate buffer for 20 minutes (Thermo Fisher Scientific, Fremont, CA; pH 6.0) at the boiling point then cooled, incubated overnight at 4°C (Anti-COX-2) (Rabbit polyclonal to COX2 1:100 (ab15191) abcam, UK) primary antibody. Followed by washing with PBS, subsequently, the slides were incubated for 30 minutes at 37°C with the biotinylated secondary antibody then with the Vector Elite ABC kit (Elite reagent Avidin DH and biotinylated horseradish peroxidase H reagents; Vector Laboratories Inc., Burlingame, CA). Then with phosphate buffered saline, the antibody-biotin-avidin-peroxidase complex was developed using diaminobenzidine tetrahydrochloride (DAB Substrate Kit; Vector Laboratories Inc.). Sections were counterstained with hematoxylin, dehydrated, and cleared in xylene then cover slipped, where the reaction seemed as a brown cytoplasmic reaction [13].

Quantitative polymerase chain reaction (qPCR)

Assessment of formalin-fixed paraffin-embedded skin specimens by qPCR was performed [14]. Reverse transcription was carried out with the SuperScript First-Strand Synthesis System for reverse transcriptase (RT)-PCR. Invitrogen's protocol was applied in the following procedure. The following ribonucleic acid (RNA)/primer 5'-3' Primer GGGGGATCTTCGGACCTCA for *P. aeruginosa* and 5'-3' primer ATGCCTGGCAGTTCC complementary to the 3' end of 5 S for rRNA *E. coli*. Each tube contained 3 μ l random hexamers and 5 μ g total RNA. The samples were incubated for 5 minutes at 65 °C then on ice for 1 minute. For each reaction, the reaction master mixture was prepared then added to the RNA/primer mixture, mixed briefly, and then placed at room temperature for 2 minutes. At each tube, 1 μ l (50 units) of Superscript II RT was added, then mixed and incubated for 10 minutes at 25 °C. The tubes were incubated for 50 minutes at 42°C, heat inactivated for 15 minutes at 70°C, and then cooled in ice. 1 μ l of RNAase was added and incubated for 20 minutes at 37 °C. The first strand complementary deoxyribonucleic acid (cDNA) was stored at -20°C till the use of RT-PCR. The primer concentrations were normalized; mixing of reverse primer pair and gene-specific was performed. The concentration of each primer (forward or reverse) was 5 pmol/ μ l. The PCR program was set up on ABI Prism standard deviation score (SDS) 7000. Setup file copy was saved, and all the PCR cycles were used for

later dissociation curve analysis. 50 °C 2 minutes, 1 cycle, 95°C 10 minutes, 1 cycle, 95°C 15 seconds → 60°C 30 seconds → 72°C 30 seconds, 40 cycles and 72°C 10 minutes, 1 cycle. After finishing the PCR, tubes were removed from the machine. The specificity of the PCR was determined by 3% agarose gel using 5 µl from each reaction. The setup file was saved, and the RT-PCR results were analyzed using SDS 7000 software

Morphometric Study

Using Leica Qwin 500 LTD (Cambridge UK) computer assisted image analyzer. The area% of homogenous material (h), inflammation (I) and vaculation (V) were measured in H&E-stained sections. The measurements were done in 10 high power fields (HPF) using interactive measurements menu. Area % of COX-2+ve cells were measured. The measurements were done in 10 HPF using binary mode in immunostained sections.

Statistical Analysis

The data obtained from different groups were compared for statistical significance using Graph Pad Prism (version 5.00). The differences among experimental groups were evaluated by one-way analysis of variance (ANOVA). Probability values lower than 0.05 ($P < 0.05$) were considered statistically significant.

Results and Discussion

Evaluation of the prepared formulae:

The prepared formulae were translucent exhibiting *Foeniculum vulgare* odor. Particle size (PS), zeta potential (ZP), polydispersity index (PDI) was measured using the technique of Dynamic Light Scattering (DLS) applied by apparatus (Zetasizer Ver. 7.11 – England). The results are shown in Table 2. Information about nanoparticles, optimal particle size and PDI is a significant requirement before their use for any treatment application. The nanoparticles charge and their repulsion to each other are measured as the ZP. Higher repulsion indicates higher stability of nanoparticles, and no agglomeration is observed [15]. The results show that the PS values are 141.6 nm for F3, 689.5 nm for F2 and 814.6 nm for F1 so increasing the surfactant amounts (span 60) plays a role in decreasing the particle size. This is due to higher ratio of span 60 to cholesterol in F3, so that the increasing in the amount of cholesterol relative to surfactant (span 60) leads to increasing PS, as in F1 and F2, this may be due to that cholesterol is a rigid molecule with an inverted cone shape. It can be intercalated between the fluid hydrocarbon chains of the surfactant when hydrated at a temperature above the gel/liquid transition temperature so increase the size of the vesicle [16]. The surfactant (span 60) composed of hydrocarbon tail chains that possess hydrophobic attraction and polar head groups that possess electrostatic repulsion [17], span 60 shows more hydrophobicity than other surfactant like span 40, span 20...etc. the more hydrophobicity of the surfactant the smaller the PS.

Table 2: PS, ZP and PDI of the Prepared Niosomes.

Formulae	F1	F2	F3
PS (nm)	814.6	689.5	141.6
ZP (mV)	-22.5	-22.5	-34.3
PDI	0.333	0.414	0.386

Niosomes size lies in the nanometric scale. They mainly composed of non-ionic surfactant of the alkyl or dialkylpolyglycerol ether class and cholesterol with subsequent hydration in aqueous media. They are made of a surfactant bilayer with its hydrophilic ends exposed on the outside and inside of the vesicle while the hydrophobic chains face each other within the bilayer. Hence, the vesicle holds hydrophilic drugs within the space enclosed in the vesicle while the hydrophobic drugs are embedded within the bilayer itself. The zeta potential examination revealed that the surface charge of all niosomes displayed negative values (-34.3 mV for F3, -22.5 mV for F2 and -22.5 mV for F1). The results revealed that F3 gave negative zeta potential values more than (-30 mV) as shown indicating stable systems [18]. The PDI indicates the sample heterogeneity based on particle size. Polydispersity occurs due to distribution of particle size in a sample, aggregation or agglomeration of the sample during analysis or isolation. International standards organizations (International Organization for Standardization) have established that PDI values < 0.05 are more common to monodisperse samples, while values > 0.7 are common to a broad size (e.g., polydisperse) distribution of particles (International Organization for Standardization standards ISO 22.412:2017 and ISO 22.412:2017). In complex matrices, it is impossible to determine the PI without significant sample preparation and NP isolation [19].

From the above results it's deduced that F3 shows the best results as it exhibits the smallest PS among the prepared formulae and will be chosen *in vivo* study. So, increasing the surfactant (span 60) amount leads to more satisfied results for PS in niosomes. The PS, ZP and PDI values of the prepared niosomes are shown in (Table 2) The PS and ZP of F3 niosome is graphically represented in (Figures 1-3) respectively. Data illustrated in (Figure 4) Revealed that *E. coli* PCR identification for 16S r DNA gene had been done for the *E. coli* identification.

Table 2: PS, ZP and PDI of the Prepared Niosomes.

Formulae	F1	F2	F3
PS (nm)	814.6	689.5	141.6
ZP (mV)	-22.5	-22.5	-34.3
PDI	0.333	0.414	0.386

Histological Results

The histopathological examination of skin tissues from control group (group I) showed normal dermis, epidermis layers with preserved architecture of sebaceous glands and hair follicle (Figure 5a,5b). While subgroup (II a) revealed moderate

to severe pathological alterations represented in disorganization in epidermal layers with multiple vacuolated areas in dermis in addition to sever congestion and dilation in blood vessels. Homogenous material in epidermis extending to dermis layer with inflammatory cell aggregates and dense neutrophilic infiltration was detected (Figure 5c-5f). Subgroup (II b) displayed moderate to mild pathological changes where fewer vacuolated areas with focal homogenous material and minute disorganization in dermis layer were seen (Figure 6a). In subgroup (II c) multiple fields of skin sections were comparable to group (I) demonstrated normal appearance and few fields of skin with less vacuolated area. (Figure 6b) Extensive pathological alterations in subgroup (III

a) were found where, all histopathological changes in subgroup (II a) were more pronounced, extensive homogenous material, remarkable loss of normal architecture with multiple vacuolated areas were evident in addition to pale area which characterized by sever neutrophilic infiltration and numerous pus cells (Figure 7a-7c). Subgroup (III b) revealed less disorganization in dermal layer, some degenerated follicle, mild separated fibers, and minute inflammatory cell aggregates (Figure 7d). In subgroup (III c) minimal changes could be detected, mild homogenous material with mild congested blood vessel and minute inflammatory cell aggregates were still observed with normal hair follicle, sebaceous glands (Figure 7e).

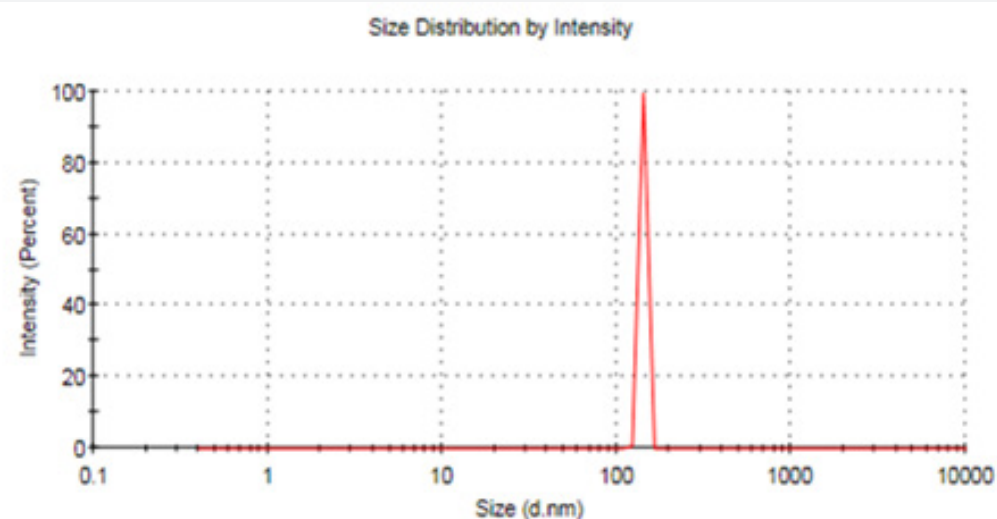


Figure 1: Particle size distribution of F3 niosome.

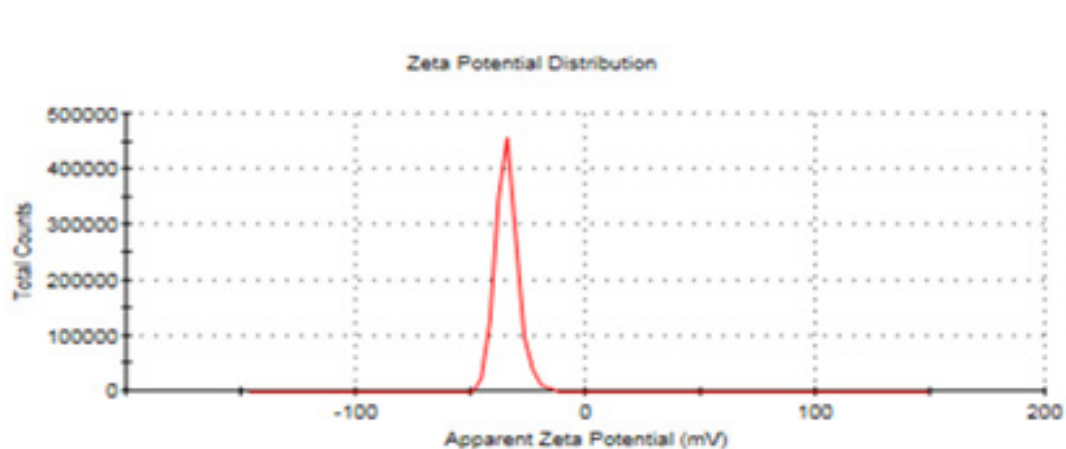


Figure 2: Zeta potential distribution of F3 niosome

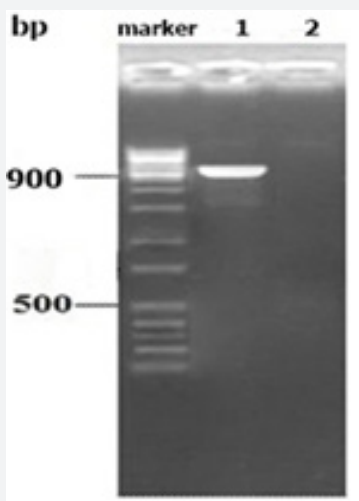


Figure 3: PCR Product Gel Electrophoresis using Agarose Gel 1 % (30 Minutes /70 Vol).
Lane marker: 100 bp DNA ladder, Lane 1: PCR product of *P. aeruginosa* (956 bp) and Lane 2: control.

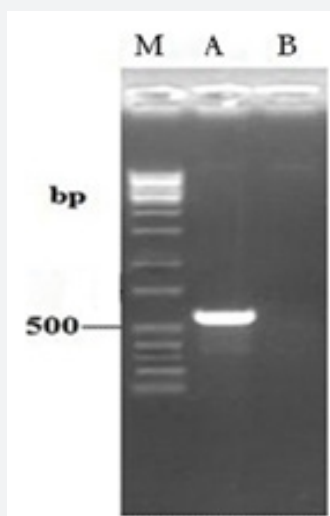


Figure 4: PCR product electrophoresis using agarose gel 1 % (70 vol).
Lane M: marker of 100 bp DNA ladder, Lane A: *E.coli* PCR product of (544 bp) and Lane B: control.

Immunohistochemical Results

The examination of immuno stained sections from Group (I) showed no immunoreactivity for COX-2 in the dermis and epidermis layers (Figure 8a). In contrast, subgroup (II a) demonstrated clear COX-2 immunoexpression in the epidermis, dermal fibers, and hair follicles (Figure 8b). Subgroup (II b) exhibited minimal COX-2 immunoexpression in the skin layers (Figure 8c), while subgroup (II c) displayed mild immunoreactivity (Figure 8d). Subgroup (III a) showed extensive immunoreactivity in both dermal and epidermal tissues. Subgroup (III b) had reduced immunoexpression, and subgroup (III c) showed minimal immunoreactivity for COX-2 in the skin tissues.

Morphometrical Results

(Table 3) and (Figure 9) showed the mean area % of homogenous material (H), inflammation (I) and vaculation (V), COX-2 immuno expression (IE) and Quantitative polymerase chain reaction (qPCR) results in experimental groups.

In this study, the mice model of abscess formation was achieved by subcutaneous injection of *E. coli* and *P. aeruginosa* into back of mice in agreement with it was reported that after a bacterial pathogen has passed through the dermal skin barrier [12], as the skin considered as first line of innate immune system is the first line of defense in the host's trial to struggle and control

infection. Animal models of *P. aeruginosa* infection in other organs have shown that neutrophils are the main cell type responsible for the primary response to *Pseudomonas aeruginosa*. The study of 21 found that highlights the normal balance between the (Type III secretions system) T3SS and host neutrophils throughout *Pseudomonas aeruginosa* abscess formation. A functional T3SS is

essential for abscess formation and for the capacity of *P. aeruginosa* to continue within the subcutaneous tissues for up to 14 days, probably by intoxicating neutrophils and inhibiting phagocytosis. Moreover, macrophages and neutrophil migrate to infection sites serve to wall off the microbes and stop its spreading in the body [13].

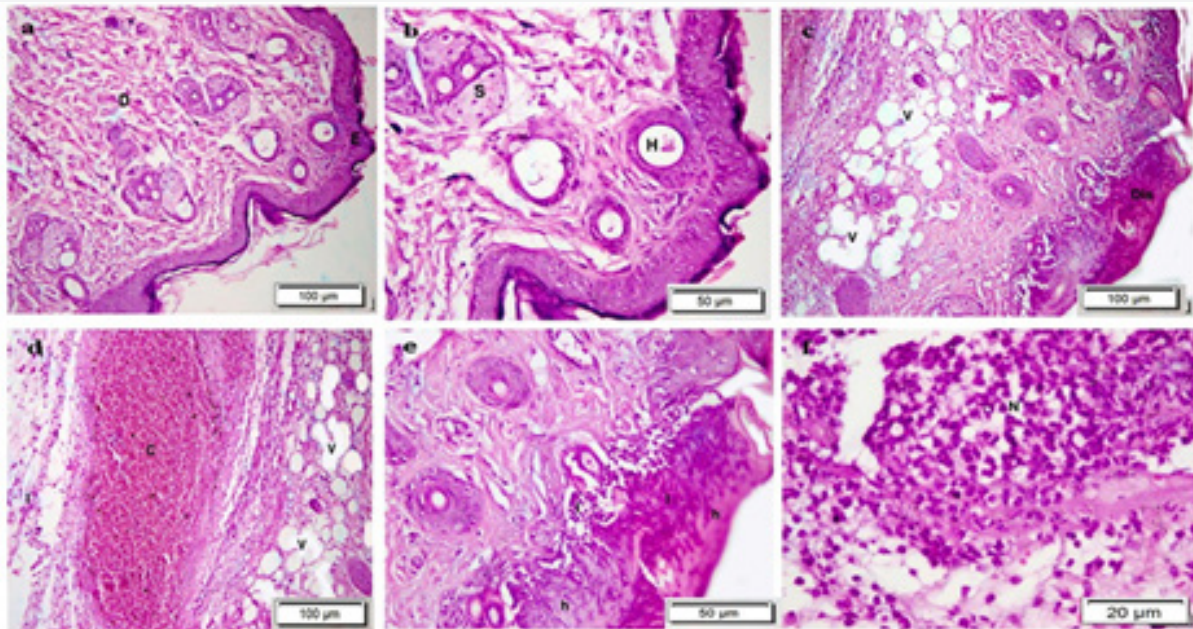


Figure 5: H&E stained sections in skin tissues. (a&b): from group I. (E): epidermis. (D): dermis. (S): sebaceous gland. (H) hair follicle. (c-f): from subgroup II a. (Dis): disorganized epidermis. (V): multiple vacuolated areas. (c): congested dilated blood vessel. (h): homogenous material. (I): cellular infiltrate. (N): dense neutrophilic infiltration. (a, c, d, x:100) (b, e, x:200) (f, x:400)

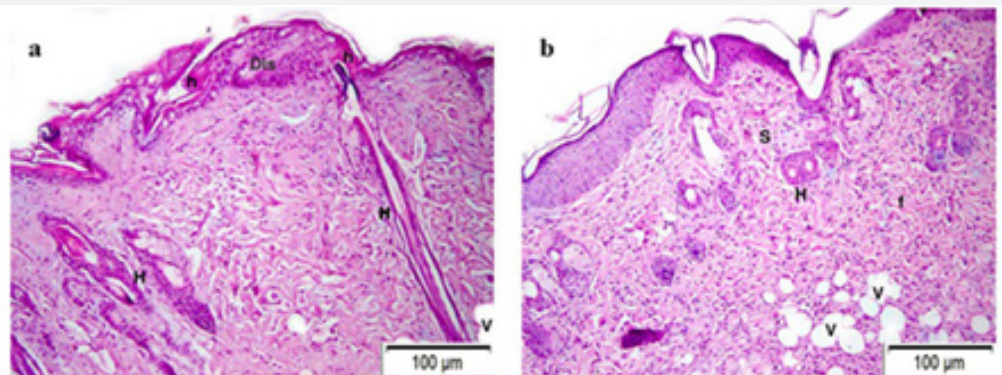


Figure 6: H&E-stained sections in skin tissues (x:100). (a): from subgroup II b. (b): from subgroup II c. (S): sebaceous gland. (H) Hair follicle. (Dis): disorganized epidermis. (V): vacuolated areas. (h): homogenous material.

Cellulitis is defined as an acute distribution of infection caused by bacteria in the skin that extends more extensively than erysipelas to reach subcutaneous tissues. While most cases

of cellulitis are caused by group A streptococcus, a number of other pathogens may cause this illness. Cellulitis due to *E. coli* is unusual and less recognized. *E. coli* and other strains that cause

extra-intestinal infections are known as extra GIT pathogenic *E. coli* [20]. Slovenian team [21] studied the virulence factor profile of *E. coli* isolated from skin and soft tissue infections (SSTI) and they deduced that these strains revealed a significant potential

virulence in comparison with strains that was isolated from urinary tract infections. However, in all cases, the entry way was cutaneous (foot leg ulcers, dermal wounds, fistulae and surgical wounds) [22].

Table 3: The mean area% of h, I, V, COX-2 immuno expression and qPCR values.

Groups and Subgroups	h area%	I area%	V area%	Cox2 area%	PCR value
Group (I)	0	0	0	0	0
Subgroup (II a)	7.9±0.4	10.2±2.1	19.8±3.2	23.4±3.1	175±10.99
Subgroup (II b)	5.1±0.7*	4.9±0.6*	8.9±1.4*	10.1± 1.9*	63±5.68*
Subgroup (II c)	2.6±0.3*	1.8±0.2*	4.1±0.7*	4.1± 0.3*	9±0.85*
Subgroup (III a)	65.9±9.1	40.8±5.3	15.3±2.5	72.5± 4.9	3506±112.30
Subgroup (III b)	30.5±2.8^	6.7±0.5^	9.2±1.3^	53.2± 5.1^	750±24.11^
Subgroup (III c)	10.1±2.1^	4.8±0.7^	7.0±1.1^	17.4± 1.8^	46±6.73^

*Significant decrease versus Subgroup (II a).

^Significant decrease versus Subgroup (III a).

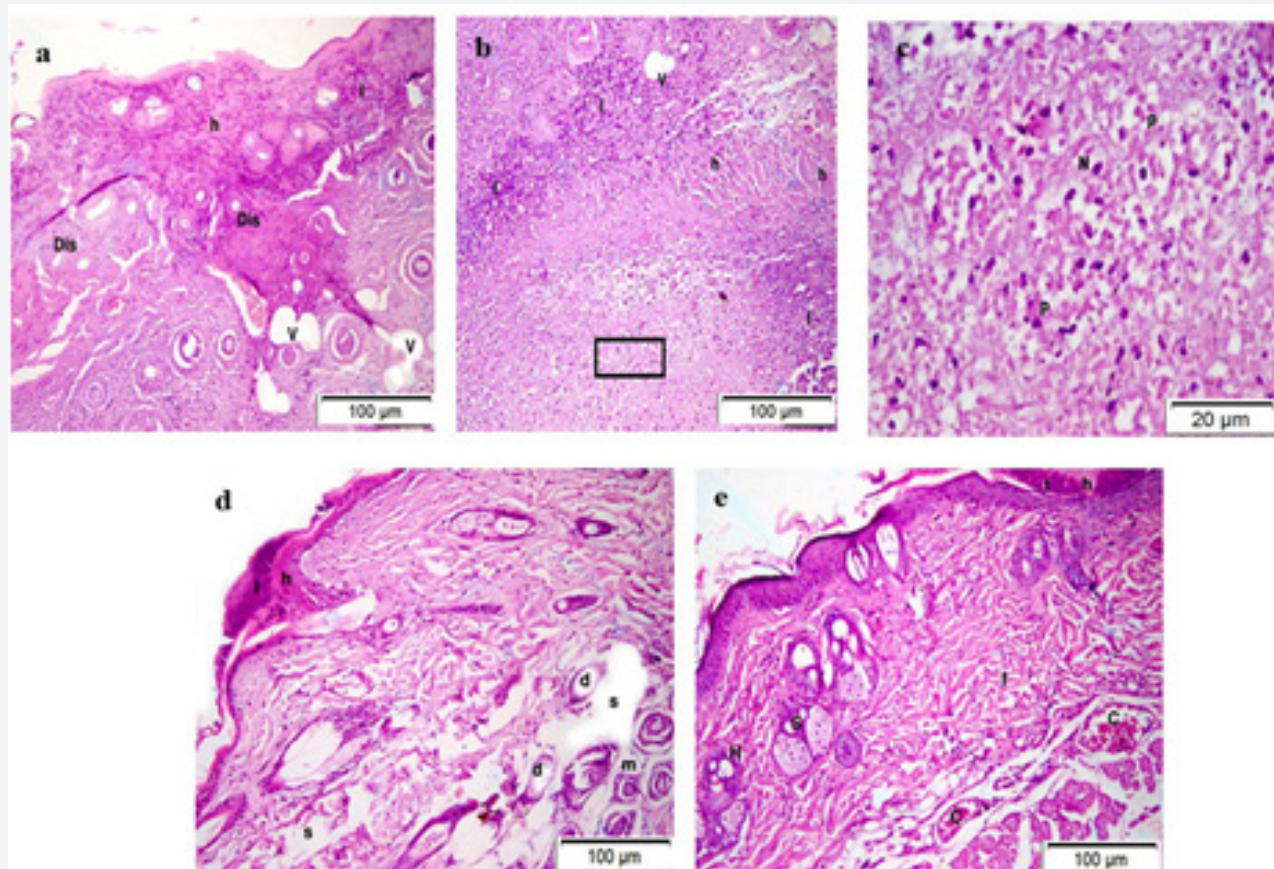


Figure 7: H&E stained sections in skin tissues. (a-c) from subgroup III a. (c) boxed area of panel (b). (d): from subgroup III b. (e): from subgroup III c. (h): homogenous material. (Dis): disorganized epidermis. (V): multiple vacuolated areas. (I): cellular infiltrate. (N): dense neutrophilic infiltration. (p): pus cells. (d): degenerated follicle. sebaceous gland. (H) hair follicle. (c): congested dilated blood vessel. (m): microfollicle. (E): epidermis. (a, b,d, e,x:100) (c, x:20)

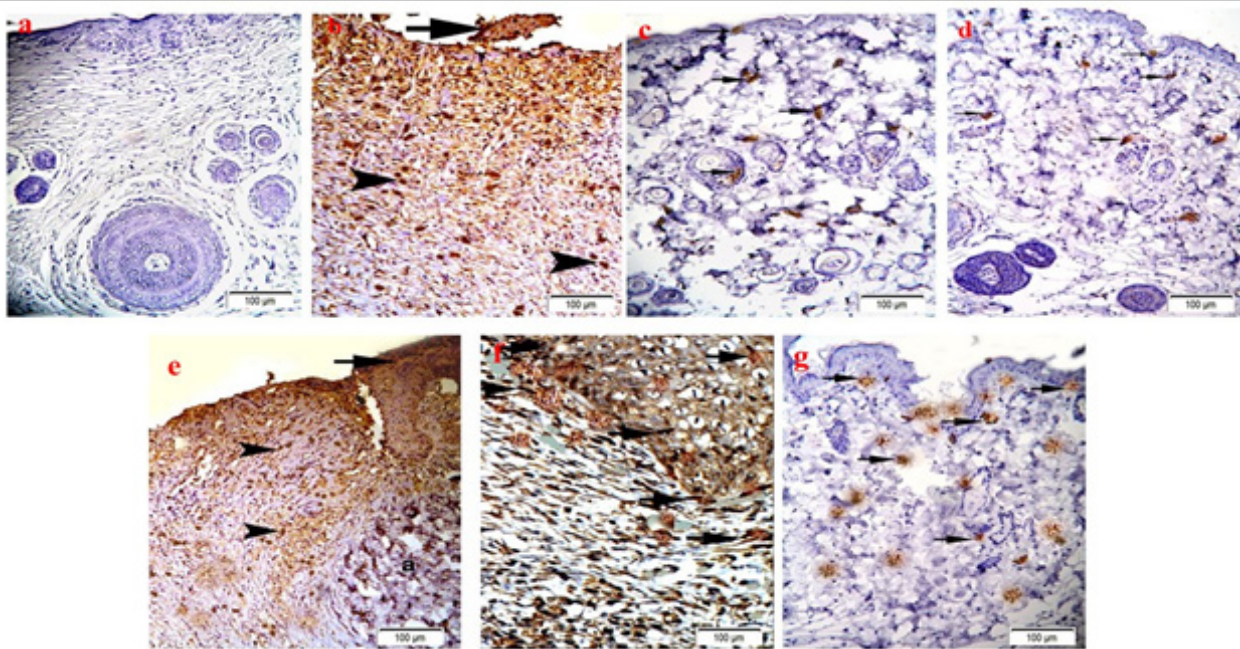


Figure 8: Cox-2 immunostained sections in skin tissues (x:100). (a): from group (I) showed -ve immunoexpression (IE) of COX-2 in dermis and epidermis layer. (b): from subgroups (II a) revealed obvious COX-2 (IE) in epidermis, dermal fiber and hair follicle. (c): from subgroup (II b) revealed minimal (IE) of COX-2 in skin layers. (d): from subgroup (II c) demonstrated mild COX-2 immunoreactivity. (e): from subgroup (III a) revealed extensive immunoreaction in dermis and epidermis tissues. (f): from subgroups (III b) showing less IE. (g): from subgroup (III c) showed minimal IE for COX-2 in skin tissues.

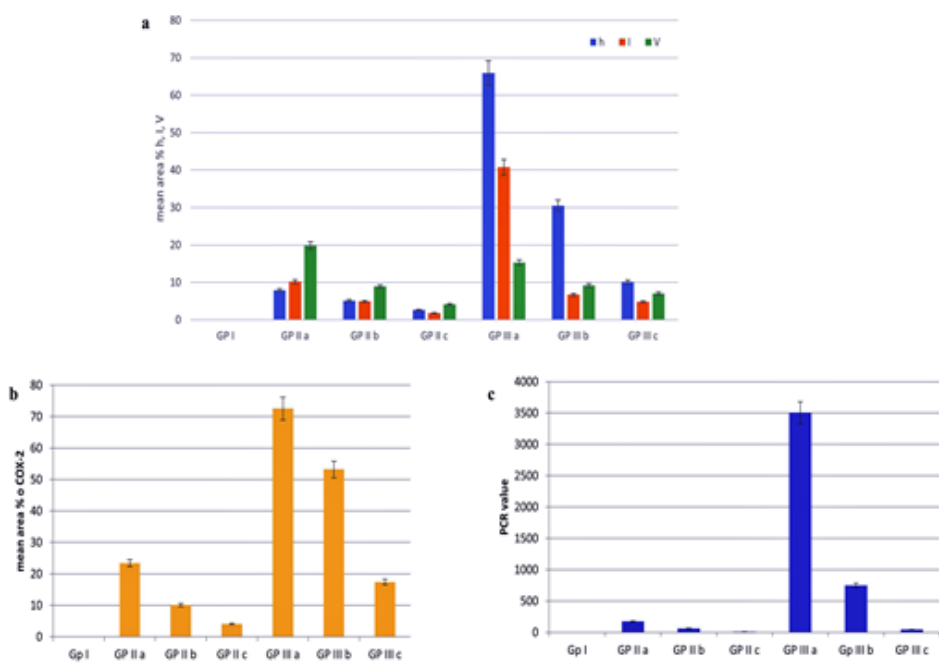


Figure 9 : (a): histogram showing the mean area % of homogenous material (h), inflammation (I) and vaculation (V), (b): histogram showing COX-2 immunoexpression (IE), (c): histogram showing Quantitative polymerase chain reaction (qPCR) results in experimental groups.

Histologically, subcutaneous injection of *E. coli* and *Pseudomonas aeruginosa* induced a pronounced pathological alteration represented in disorganization in epidermal layers with multiple vacuolated areas in dermis in addition to sever congestion and dilation in blood vessels. Homogenous material (exudate) due to deposition of fibrin in epidermis extending to dermis layer with inflammatory cell aggregates and dense neutrophilic infiltration numerous pus cells were detected. These results were confirmed by morphometric assessment which indicates a significant increase in mean area % of homogenous material (h), inflammation (I), vaculation (V) and qPCR values in infected groups compared to control group. These results are in consistent with [23] who documented that *E. coli* is a Gram -ve bacterium hardly found on the dermal skin. However, *E. coli* strongly stimulates expression of s100 A15 (a member of s 100 protein) in vivo and in vitro. This is action is mediated by toll like receptor 4 (TLR4). These proteins play a vital role in the pathogenesis of several dermal diseases. On the other hand, the damaged tissue and pathogenic microorganisms' combination produces infiltration in immune cells and assists mature abscess formation. Invading of pathogenic bacteria is known early through SSTI by dermal keratinocytes and resident dermal monocytes that initiate interleukin signaling to stimulate immune cell recruitment [24]. That prompts the entrance of neutrophils to the infection area forming abscess formation process. Also, the neutrophils invasion leads to amplified blood vessels permeability at the inflammation site. The clumping factor A and coagulases function are mainly through binding or modifying plasma glycoprotein, mainly fibrinogen. Fibrin deposition is a critical process to abscess formation and contributes to defense of host against invading bacteria [25].

Infected groups showed numerous +ve COX-2 cells were evaluated and significantly increased in the mean area percentage of +ve IE. Illustrated previous results indicated an increase in inflammation. It was stated that PGs produced by COX-2 are involved in pathological conditions like inflammation, loss of function, pain, hotness, fever, wound repair, angiogenesis, increased vascular permeability and vasodilation [26]. On the other hand, treated groups showed significant decrease in COX-2 immuno expression. Studies have revealed that COX-2 stops much of the skin damage prompted by acute UV exposure. Topical therapy of SKH-1 mice with celecoxib directly after only exposure to UVB irradiation was shown to reduce significantly UV-induced skin dermal neutrophil infiltration, edema, and activation (induction of myeloperoxidase activity), number of p53-positive cells, dermal proliferation and oxidative DNA damage [27].

In the present study, the treatment of infected groups with *Foeniculum vulgare* oil especially it's niosome form resulted in notable restoration of skin tissues, in agreement with [28] who documented that methanol extract of *Foeniculum vulgare* reduce inflammation via cyclo-oxygenase and lipoxygenase pathways. The application of niosomal technology is widely varied and can

be used to target drugs to site of action. This proof the high anti-inflammatory effect of fennel niosome. Anti-inflammatory activity of *Foeniculum vulgare* essential oil is mediated by the prevention of pro-inflammatory cytokines such as IL-6 and TNF- α expression in chronic obstructive pulmonary disease mouse model [29]. It is well recognized that trans-anethole, fenchone and D-limonene are the main constituent of essential oil of *Foeniculum vulgare*, trans-anethole have protective effect against hepatic I/R injury by the downregulation of release of IRF-1-mediated HMGB1 and consequently NF- κ B and TLR activation [30]. Also, fenchone decrease the inflammatory cells count during healing of dermal wound in the experimental model of skin wound healing [31]. In another study, d-limonene withdrawn the inflammation and oxidative stress induced by doxorubicin through suppress the expression of COX-2, NF- κ B and iNOS in the kidney of wistar rats [32]. Additionally, limonene had pronounced anti inflammatory effect by decreasing IL-1 β , JNK, NF- κ B and p38 activation [33].

Conclusion

From the above results it is deduced that both niosome formula and *Foeniculum vulgare* oil exhibits anti-inflammatory activity but niosome formula shows more efficacy than *Foeniculum vulgare* oil, this may be due to niosome as a formula possesses smaller particle size than a raw material alone (*Foeniculum vulgare* oil) which has a main role in drug penetration and absorption in the site of application thus, facilitated macrophages migrate toward site of infection killing pathogenic bacteria.

References

1. Fredricks DN (2001) Microbial Ecology of the Human Skin in Health and Disease. *J Investig Dermatol Symp Proc* 6(3): 167-169.
2. Chiller K, Selkin BA, Murakawa GJ (2001) Skin Microflora and Bacterial Infections of the Skin. *J Investig Dermatol Symp Proc* 6(3): 170-174.
3. Singer AJ, Talan DA (2014) Management of skin abscesses in the era of methicillin-resistant *Staphylococcus aureus*. *The New England Journal of Medicine* 370(11): 1039-1047.
4. Cox CT, Jeffrey SD, Medical Illustrations, Birck (2007) *The encyclopedia of skin and skin disorders*. (3rd ed.). New York, NY: Facts on File p. 1.
5. Dryden MS (2010) Complicated Skin and Soft Tissue Infection. *J Antimicrob Chemother* 65(Suppl 3): 35-44.
6. Owens CD, Stoessel K (2008) Surgical Site Infections: Epidemiology, Microbiology and Prevention. *J Hosp Infect* 70(Suppl 2): 3-10.
7. Lessnau KD, Cunha BA, Dua P (2012) *Pseudomonas aeruginosa* Infections.
8. Bjarnsholt T, Kirketerp-MK, Jensen PO (2008) Why Chronic Wounds Will Not Heal: A Novel Hypothesis. *Wound Rep Reg* 16: 2-10.
9. Rouzer CA, Marnett LJ (2003) Mechanism of free radical oxygenation of polyunsaturated fatty acids by cyclooxygenases. *Chemical reviews* 103(6): 2239-2304.
10. Nurmi JT, Puolakkainen PA, Rautonen NE (2005) *Bifidobacterium Lactis* sp. 420 up-regulates cyclooxygenase (Cox)-1 and down-regulates Cox-2 gene expression in a Caco-2 cell culture model. *Nutrition and cancer* 51(1): 83-92.

11. Heard CM (2020) An ex vivo skin model to probe modulation of local cutaneous arachidonic acid inflammation pathway. *Journal of Biological Methods* 7(4): e138.
12. Aboul Fotouh GI, Zickri MB, Metwally HG, Ibrahim IR, Kamar SS, et al. (2015) Therapeutic effect of adipose derived stem cells versus atorvastatin on amiodarone induced lung injury in male rat. *Int J Stem Cells* 8: 170-180
13. Bassiony HS, Zickri MB, Metwally HG, Elsherif HA, Alghandour SM, et al. (2015) Comparative histological study on the therapeutic effect of green tea and stem cells in Alzheimer's disease complicating experimentally induced diabetes. *Int J Stem Cells* 8: 181-190.
14. Pu T, Guo P, Qiu Y, Chen S, Yang L, et al. (2015) Quantitative real-time polymerase chain reaction is an alternative method for the detection of HER-2 amplification in formalin-fixed paraffin-embedded breast cancer samples. *Int J Clin Exp Pathol* 8: 10565-10574.
15. Rajesh Jain, Hemali Savla, Isha Naik, Jinesh Maniar, Kapil Punjabi (2018) Handbook of Nanomaterials for Industrial Applications pp. 587-620.
16. Abdelkader H, Farghaly U, Moharram H (2014) Effects of surfactant type and cholesterol level on niosomes physical properties and in vivo ocular performance using timolol maleate as a model drug. *J Pharm Investig* 44(5): 329-337.
17. Tanford C (1973) The Hydrophobic effect: formation of micelles and biological membranes. Wiley, New York.
18. Darwish A (2016) Increasing the activity and safety of the anti-inflammatory drug lornoxicam via niosomal encapsulation. p. 13-14.
19. Thilak Mudalige, Haiou Qu, Desiree Van Haute, Siyam MA, Angel Paredes, et al. (2019) Nanomaterials for Food Applications pp. 313-353.
20. Rangel S M, Diaz M H, Knoten C A, Zhang A, & Hauser A R, et al. (2015) The role of ExoS in dissemination of *Pseudomonas aeruginosa* during pneumonia. *PLoS pathogens* 11(6): e1004945.
21. Berube BJ, Murphy KR, Torhan MC, Bowlin NO, Williams JD, et al. (2017) Impact of type III secretion effectors and of phenoxyacetamide inhibitors of type III secretion on abscess formation in a mouse model of *Pseudomonas aeruginosa* infection. *Antimicrobial agents and chemotherapy* 61(11): e01202-17.
22. Stevens DL, Bisno AL, Chambers HF, Everett ED, Dellinger P, et al. (2005) Practice guidelines for the diagnosis and management of skin and soft-tissue infections. *Clinical Infectious Diseases* 41(10): 1373-1406.
23. Petkovsek Ž, Eleršič K, Gubina M, Žgur Bertok D, Erjavec MS, et al. (2009) Virulence potential of *Escherichia coli* isolates from skin and soft tissue infections. *Journal of clinical microbiology* 47(6): 1811-1817.
24. Sunder S, Haguenoer E, Bouvet D, Lissandre S, Bree A, et al. (2012) Life-threatening *Escherichia coli* cellulitis in patients with haematological malignancies. *Journal of medical microbiology* 61(9): 1324-1327.
25. Büchau AS, Hassan M, Kukova G, Lewerenz V, Kellermann S, et al. (2007) S100A15, an antimicrobial protein of the skin: regulation by *E. coli* through Toll-like receptor 4. *Journal of Investigative Dermatology* 127(11): 2596-2604.
26. Funk CD (2001) Prostaglandins and leukotrienes: advances in eicosanoid biology. *science* 294(5548): 1871-1875.
27. Rundhaug JE, Fischer SM (2008) Cyclo-oxygenase-2 plays a critical role in UV-induced skin carcinogenesis. *Photochemistry and photobiology* 84(2): 322-329.
28. Kooti W, Moradi M, Ali-Akbari S, Sharafi-Ahvazi N, Asadi-Samani M, et al. (2015) Therapeutic and pharmacological potential of *Foeniculum vulgare* Mill: a review. *Journal of HerbMed Pharmacology* 4(1): 1-9.
29. Kim KY, Lee HS, Seol GH (2017) Anti-inflammatory effects of trans-anethole in a mouse model of chronic obstructive pulmonary disease. *Biomedicine & Pharmacotherapy* 91: 925-930.
30. Cho HI, Kim KM, Kwak JH, Lee SK, Lee SM, et al. (2013) Protective mechanism of anethole on hepatic ischemia/reperfusion injury in mice. *Journal of natural products* 76(9): 1717-1723.
31. Keskin I, Gunal Y, Ayla S, Kolbasi B, Sakul A, et al. (2017) Effects of *Foeniculum vulgare* essential oil compounds, fenchone and limonene, on experimental wound healing. *Biotechnic & Histochemistry* 92(4): 274-282.
32. Rehman MU, Tahir M, Khan AQ, Khan R, Oday-O-Hamiza, et al. (2014) D-limonene suppresses doxorubicin-induced oxidative stress and inflammation via repression of COX-2, iNOS, and NF κ B in kidneys of Wistar rats. *Experimental biology and medicine* 239(4): 465-476.
33. Rufino AT, Ribeiro M, Sousa C, Judas F, Salgueiro L, et al. (2015) Evaluation of the anti-inflammatory, anti-catabolic and pro-anabolic effects of E-caryophyllene, myrcene and limonene in a cell model of osteoarthritis. *European journal of pharmacology* 750: 141-150.



This work is licensed under Creative Commons Attribution 4.0 License
DOI: [10.19080/GJPPS.2024.11.555821](https://doi.org/10.19080/GJPPS.2024.11.555821)

Your next submission with Juniper Publishers
will reach you the below assets

- Quality Editorial service
- Swift Peer Review
- Reprints availability
- E-prints Service
- Manuscript Podcast for convenient understanding
- Global attainment for your research
- Manuscript accessibility in different formats
(Pdf, E-pub, Full Text, Audio)
- Unceasing customer service

Track the below URL for one-step submission
<https://juniperpublishers.com/online-submission.php>